Scanning Microscopy Vol. 12, No. 4, 1998 (Pages 585-598) 0891-7035/98$5.00+.25
Scanning Microscopy International, Chicago (AMF O'Hare), IL 60666 USA

MEASUREMENTS OF MECHANICAL PARAMETERS OF BIOLOGICAL STRUCTURES WITH ATOMIC FORCE MICROSCOPE

Atsushi Ikai*, Xue-Ming Xu and Keita Mitsui

Laboratory of Biodynamics, Tokyo Institute of Technology,
Nagatsuta, Midoriku, Yokohama, Japan 226

(Received for publication March 21, 1996 and in revised form March 20, 1997)

Abstract

Atomic force microscopy has been increasingly used for the measurement of mechanical parameters of biological materials in addition to imaging them. This article reviews recent contributions to the development of the methods used for such measurements and reliable interpretations of the data obtained. Kinds of mechanical properties that have attracted the attention of users of atomic force microscope include Young's modulus, binding force between single pairs of ligands and receptors, antigen and antibody binding, internal cohesive force of protein molecules, and the force of base pairing in double helical DNA. The mechanical manipulation of soft (or compliant to be exact) biological materials with atomic force microscope has also been attempted on chromosomes, cells, and DNA. Some of the recent work in chromosomal manipulation will be reviewed.

Key Words: Atomic force microscope, force curves, mechanical parameters, proteins, chromosomes, biological structures.

*Address for correspondence:
Atsushi Ikai, address as above.
Telephone number: 81 45 924 5828
FAX number: 81 45 924 5806
E-mail: aikai@bio.titech.ac.jp

Introduction

The impact of atomic force microscopy (AFM) on biologically oriented research fields has been increasingly felt as ever wider applications of the method are being reported. Imaging soft (or compliant to be exact) biological samples under near-native conditions in aqueous environment has been one of the strong points of the AFM method as compared to the electron microscopy (EM) methods [17, 18, 21, 31, 43, 55] although the resolution of the latter is still much better than that of AFM. The resolution of AFM itself is now at an atomic level and comparable to that of EM [58] but when it is applied on biological samples, the resolution is severely limited by a large loading force and the sample compliance [44]. The tip may press, drag, or pull the sample surface and, sometimes, it may penetrate into the sample interior by breaking the surface structure, thus contributing to the deterioration of the resolution. The very problems we have just mentioned are actually the most attractive aspects of the AFM technology to many researchers who are now using this instrument to measure the mechanical parameters of the biological samples and often to manipulate them for revealing new aspects of them. In this article, we will review applications of AFM to the measurements of: (1) Young's modulus of fibers and gel-like materials including chromosomes; (2) interaction force between ligands and receptors, including that of antigens and antibodies; (3) intramolecular cohesive energy of protein molecules; and, (4) the base pair interactions in double stranded DNA. Then, we will comment on the importance of the direct measurement of the spring constant of the cantilever and possible interpretation of unusual force curves reported in the literature.

Experimental Results

Young's modulus

The elastic property of isotropic material may be represented by two elastic constants, and Young's modulus, E, and Poisson's ratio ν are often chosen for convenience. Then the rigidity modulus, G, is given as

$$G = E/2(1 + \nu) \quad (1)$$

A commonly employed procedure of forming an indentation on an infinitely flat surface of test material and measuring the depth of indentation as a function of the applied force may be represented in Figure 1 as adapted from Pharr [41].

Generally speaking, since a given test material has both elasticity and plasticity, the loading part of the curve is not superimposable with the unloading part. The tangent of the unloading curve at the beginning of unloading is then used to obtain the reduced Young's modulus with $E^* = E/(1-\nu^2)$ (when the indenter can be assumed as undeformable, and

$$1/E^* = (1 - \nu_1^2)/E_1 + (1 - \nu_2^2)/E_2$$

when both tip and the sample are deformable).

$$\frac{dP}{dh} = \frac{2\,E^*\sqrt{A}}{\sqrt{\pi}} \quad (2)$$

where h, P, and A represent, respectively, the depth of indentation, the applied force, and the area of contact between the tip and the test material [41]. Evaluation of contact area, A, is though difficult when the tip is small.

Such difficulty can be alleviated when the sample is elastic and the loading and unloading curves are superimposable within experimental errors, because integrated equations relating the depth of indentation and the applied force may be used without requiring the contact area. Luckily, examples of biological materials so far reported, namely, chitin fiber, gelatin gel, and acid treated chromosomes, have been noted to be largely elastic with little plasticity when the load was not very large. Representatives of such equations are given below for two types of indenter [56]. First, for a conical indenter of "semivertical angle" of α, the force P is proportional to the 2nd power of the depth of indentation, *D*.

$$P = \frac{4\,G\cot\alpha}{\pi(1-\nu)}\,D^2 \quad (3)$$

There are occasional misquotations of this formula by equating a to the opening angle of the cone or half of it (in that case, cota in the above equation should be replaced with tana), but according to the derivation by Sneddon [56], it is meant to represent the angle a as depicted in Figure 2.

Second, for a paraboloidal indenter with an effective radius of curvature of 2k at the tip, P is related to D in the following way:

$$P = \frac{8G}{3(1-\nu)}\left(2kD^3\right)^{1/2} \quad (4)$$

In both cases, as mentioned above, numerical values that can be obtained from the experiment are $G/(1-\nu)$ or $E/2(1-\nu^2)$ rather than *E* itself. It is, therefore, not possible to extract the numerical value of Young's modulus without the knowledge of Poisson's ratio. Since the latter is commonly in the range of 0.3-0.5, Young's modulus may still be estimated within an ambiguity of ± 10% without direct knowledge of Poisson's ratio. For compliant materials, ν is in the range of 0.4-0.5, examples are: gold (0.44), lead (0.44), polyethylene (0.46), and elastic rubber (0.46-0.49) [38].

As there is a growing interest among material scientists to use micro- to nanometer sized indenters to probe the elastic properties of small samples as well as those of small area of large samples, re-evaluation of indentation experiment has been attempted from several fronts, such as: (1) numerical correction of the relation between P and D for non-axisymmetric indenters, and, (2) incorporation of finite sharpness of the tip at its apex [19, 25, 40]. When AFM is used as a nanoindenter, it is most likely that a commercially available pyramidal tip is used for which no exact relation between P and D is available. Approximation of tip shape by a cone or a paraboloid is therefore necessary. Moreover, the sample surface of biological specimens may not be perfectly flat even for a short distance, and, in many commercially available AFM instruments, the cantilever approaches the sample surface with a fixed angle of approximately 10°. Although the latter factor may be alleviated in the future, flatness of biological specimens cannot be guaranteed. Therefore, there is another source of approximation when equations, such as given above, are used for the analysis of indentation experiments.

Despite such ambiguities in the determination of Young's modulus from indentation experiments, it is remarkable that AFM allows us to measure the mechanical properties of nanometer sized biological specimens for the first time. Instrumental modifications to minimize some of the ambiguities mentioned above would not be difficult once the importance of such measurement is recognized. According to the literature cited above, numerical factors correcting for the tip shape do not exceed the experimental ambiguities on biological samples at the present stage.

The use of AFM for the measurement of sample rigidity was first reported by Burnham and Colton [4] who were followed by Tao *et al*. [59], Xu *et al*. [65] and Radmacher *et al*. [45, 46, 47]. Tao *et al*. [59] measured the microelastic properties of three different samples, namely, stainless steel, bone, and rubber using the force versus distance mode of AFM. The rigidity constant of the rubber used in the AFM experiment was calibrated with a

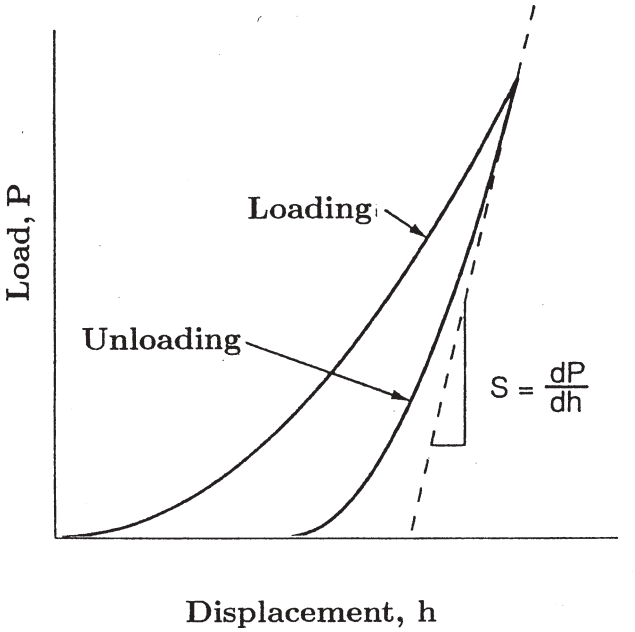

Figure 1. The typical shape of loading and unloading curve in an indentation experiment. When the sample material displays no plasticity, the unloading curve coincides with the loading curve.

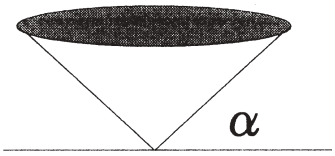

Figure 2. Definition of "semivertical" angle α in one of Sneddon's formulae.

macroscopic apparatus, giving a value of 1.1 x 10^7 Pa for $G = E/2(1 + \nu)$. The analysis of AFM force curves gave a G value of 1.3 x 10^7 Pa for the same rubber. Agreement between the two experiments was good and provided yet another way to calibrate the force constant of a cantilever.

Xu *et al*. [65] pushed a β-chitin fiber of several μm long with AFM tip and measured the deflection of the cantilever and the bend of the fiber. The fiber was placed over the surface of GaAs grating with grooves of 300, 500, 700 nm wide and 300 nm deep. A test chitin fiber was suspended over several grooves. There was a problem of whether the parts of the fiber in contact with the ridges were free to be moved or not, when the suspended part of the fiber was bent. In their application of beam bending model, the authors assumed that the ends of the fibers were fixed. The location of the fiber was identified by scanning with AFM, and the position of force application was selected from the AFM image of the fiber. The cantilever was calibrated for its spring constant from its resonance frequency. The Young's modulus of a fiber with cross sections less than 20 nm x 40 nm was determined as 1-2 x 10^{11} Pa. They also measured the elastic modulus of S-layer sheath of archaeobacterium, *M. hungatei* and within an isotropic assumption, obtained a Young's modulus of 1-3 x 10^{10} Pa. The threshold value of applied force to cause a plastic deformation on the S-layer sheath was investigated.

Radmacher *et al*. [46] recorded force curves to measure the rigidity of protein molecules (lysozyme) adsorbed on the mica surface and came up with the value of 0.5 ± 0.2 x 10^9 Pa, which was in agreement with the value obtained with macroscopic method of compressibility of protein crystals. They extended their measurements to gelatin gels in water and propanol [47]. Gelatin gel is a macroscopic model but the measurement of its local elastic modulus was of some interest. The success of the method was extended by Ikai *et al*. [24] to the measurement of elastic properties of microscopic structures such as chromosomes.

Ikai *et al*. [24] measured the rigidity of acid-treated human chromosome as the first example of subcellular organelles. Although the acid-treated chromosomes are no longer biologically active, such samples are widely used in the field of chromosome study including the fluorescent *in situ* hybridization method (FISH). The study of the mechanical properties of acid-treated chromosomes is useful in our work to extract small amounts of DNA from finely targeted areas of individual chromosomes. Cells from G-401 cell line derived from a kidney tumor of a three-month old male Caucasian were grown in McCoy's 5A medium with 10% fetal calf serum. Cells were exposed to colcemid (0.05 μg/ml) and arrested at the mitotic stage. Mitotic cells were harvested and treated with 75 mM KCl at 37°C for 15 minutes, followed by fixation with methanol: acetic acid (3:1 v/v) solution. One drop of cell suspension was spread onto a clean glass cover-slip 15 mm in diameter, and the sample was air-dried or submerged under an aqueous buffer after washing.

Measurement of the rigidity of chromosomes in buffer solution was conducted according to Radmacher's method on gelatin gels with a calibrated cantilever for its spring constant. The buffers used in experiments were as follows: (1) 50 mM phosphate buffer with 0.1 M NaCl at pH 7.0; (2) 0.15 M acetate buffers with pH from pH 7.0 to 2.0. The pH of extreme ends of buffer function was adjusted by the addition of either concentrated NaOH or HCl. For experiments at high pH, 0.15 M bicarbonate buffer of pH 10.6 was used. The temperature was 25°C. The measurement of Young's modulus depended primarily on the pH and the ionic concentration of the solvent and not so much on the type of buffers.

The loading and unloading parts of the force curves

obtained in neutral pH were superimposable, as shown in Figure 3, within experimental errors, suggesting that the chromosomes could be approximated as elastic substance. The rigidity was not noticeably different over various areas of chromosomes, or with the change of pH between 10.5 and 6, but it showed a ten fold increase in the Young's modulus when the pH of the buffer was decreased to 4.1. The Young's modulus was calculated based on an arbitrary value of 0.4 for the Poisson's ratio. The Young's modulus decreased again at pH 2 [64]. The result is summarized in Table 1.

There was a significant decrease in the height of the chromosome along with the observed increase in the Young's modulus. We think that the protonation of DNA in the chromosome as cited below decreased the electrostatic repulsion within the chromosome leading to a drastic decrease in its volume and consequently to the increase in rigidity.

Imaging of chromosomes immediately before or after force curve measurements showed a drastic decrease in the apparent height and width of the chromosomes in a pH 3-4 range, and the chromosome surface showed strong adhesive interactions towards silicon nitride tips as shown in Figure 3. It is interesting to notice that DNA has its isoelectric point in the pH range of 3-4 [26]. It is reasonable to assume that the reduction of net charge on DNA increased the interaction between chromosome and the tip. It was verified that pure plasmid DNA which was physisorbed on mica surface became sticky towards the AFM tip in a mildly acidic solution of pH 3-4. The result strongly suggested that the sticky material in the chromosome was DNA. The force curves obtained under the experimental conditions where the chromosome surface showed stickiness was apparently not superimposable for the loading and unloading parts. In such cases, the Young's modulus obtained from the loading part of the curve should be regarded as approximate ones.

Complicated force curves with multiple deflections have been discussed by Aimé *et al*. [1], both theoretically and experimentally in relation to the force measurement on polymer films. In the case of polymer films, the multiple deflections were interpreted as occurring from the cracks or fractures created on the bulk or the contact area between the film and the tip. Since, in the case of chromosome immersed in water, it is rather unlikely that cracks would have developed during the force curve measurement, we think the situation is quite different from the polymer films. We interpret such force curves obtained in our experiment as representing stretching of the sandwiched samples in response to the tensile force from the deflected cantilever. The shape of the force curve may depend on the time scale of cantilever movement because, unlike thermodynamics, mechanics generally depends on time. An informative

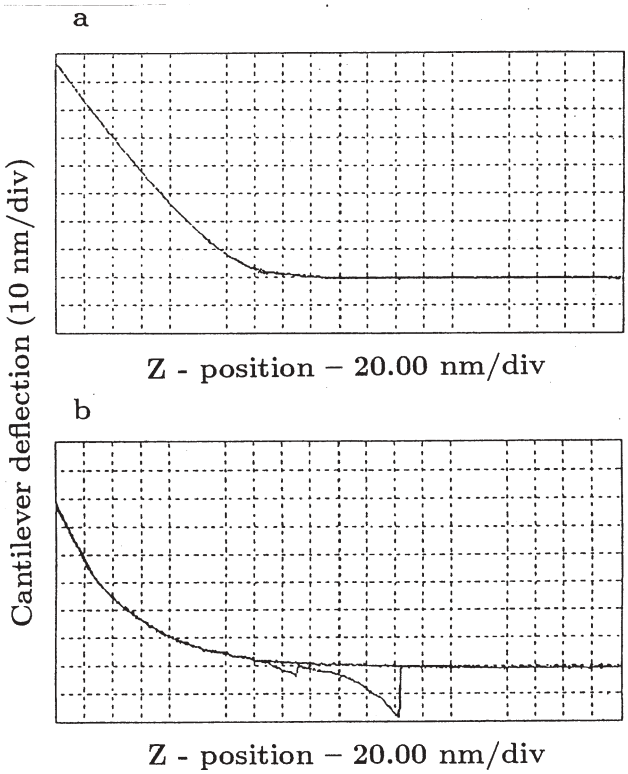

Figure 3. Force curves obtained on: (**a**) a surface of chromosome at a neutral pH, and (**b**) a sticky chromosome under mildly acidic solutions.

example may be found in the field of adhesion. Using a molecular dynamics simulation, Baljon and Robbins [2] studied the time dependence of rupture force between two surfaces in contact with adhesive bonds. The required force was observed to increase with the rate of rupture but asymptotically reached a plateau value when the tearing rate was slow. Since the force experiment using AFM technology operates at very slow time constants, it is probably safe to assume that most of the reported force values in the cited literature are in the plateau region. But, in some cases, biological materials have shown time dependent mechanical properties. Such viscoelastic properties of cells have been the subject of active researches [22, 44]. For example, Radmacher *et al.* [44] investigated the viscoelastic properties of cytoskeleton of human platelet cells by analyzing the dependence of the shape of the force curve on the rate of force curve measurement. The soft cantilever they used (spring constant = 0.03 N/m) was found to be dragged by solvent when the scan rate was as high as 20 Hz, but the response from platelets was largely undisturbed. They concluded that cells behaved elastically within their experimental conditions.

Table 1. Estimated Young's modulus of human chromosomes.

Solvent pH	*Young's Modulus (Pa)*
10 mM phosphate buffer with 0.15 M NaCl at pH 7.4	$0.8 \pm 0.3 \times 10^5$
10 mM bicarbonate buffer with 0.15 M NaCl at pH 10.6	$0.6 \pm 0.3 \times 10^5$
10 mM acetate buffer with 0.15 M NaCl at pH 4.1	$13 \pm 4 \times 10^5$

The increase of Young's modulus in some cases may be related to the volume change of the sample gels. According to the treatment of Treloar [60], the rigidity modulus of cross-linked gels, G, is related to the volume fraction of gel material, ν_2, through the following equation,

$$G = (RT/V_1)\{(1/2)-\chi\}\nu^{/3} \quad (5)$$

where V_1 is the molar volume of the solvent, and χ is an adjustable parameter in the original Flory-Huggins treatment of polymer solutions. Since ν_2^{-1} is proportional to the degree of swelling, the equation predicts that Young's modulus varies with -5/3 power of the swelling ratio. It will be interesting to test the validity of the power dependence of rigidity on swelling for gel-like biological specimens, although it has been reported that a quantitative application of the above equation was difficult when water was the solvent.

Ligand-receptor interactions

Lee *et al*. [28] and Florin *et al*. [11] were the first to demonstrate that AFM could be used to measure the binding force between the ligand and receptor molecules. These papers have been reviewed extensively by other authors, and we will not go into the details here except to emphasize that the papers opened a new field of force measurement in biochemistry where thermodynamics had been, and still is, prevailing. For the purpose of molecular manipulations using biological molecules, such as proteins, carbohydrates and nucleic acids, mechanical parameters will be regarded as important as thermodynamical parameters.

Recently, the force required to disrupt the binding between an antigen-antibody pair was measured. Dammer *et al*. [8] carefully coated the substrate and cantilever with organic molecules and biotin antigens were derivatized at the end of the 2 nm long cross-linker, and the latter was cross-linked to bovine serum albumin which was linked to the organic layer on the tip. The long cross-linker allowed substantially free orientation of antigens to combine with antibodies. Antibodies were covalently linked to the substrate that was coated with organic layers. Then, the force curves were measured in buffer solution by repeatedly bringing the tip and the substrate into contact.

Dammer *et al*. [8] analyzed the magnitude of the final jump of the cantilever from the downwardly deflected position to the horizontal baseline in line with the analysis carried out by Florin *et al*. [11]. The value of 120 pN was suggested as the unbinding force between a single binding pair but there was no claim of directly measuring the force of a single pair unbinding. Their careful procedure for functionalizing the tip and the substrate for immobilizing antigens and proteins were impressive. It is important to take precautions to retain the motional freedom of ligand molecules as much as possible and take similar precautions to keep proteins as native as possible on a solid surface of substrate such as mica, gold or glass.

Hinterdorfer *et al*. [20] used a 6 nm long cross-linker to harness antibodies and antigens (human serum albumin), respectively to the activated surface of silicon substrate and tip. The very long arm of the polyethylene glycol based cross-linker allowed efficient search for binding partners resulting in nearly 50% in the success rate of recording downwardly deflecting force curves suggesting antigen-antibody binding. They analyzed the magnitude of the force at the final release and obtained the value of 244 ± 22 pN for the unbinding force of a single antigen-antibody pair. Stretching of sensor was limited to less than 30 nm and could be accounted for by an almost full extension of the polyethylene glycol parts. The value cited by the authors as the unbinding force was larger than the force of 160 pN obtained by Florin *et al*. [11] for a single pair unbinding of biotin and avidin. From the value of binding constants, the biotin-avidin system is by far the most stable ligand-receptor pair in biochemistry, therefore, the result that indicated a stronger binding for antigen-antibody was rather surprising.

There is no simple theoretical relation between the binding constant and unbinding force but attempts have been made to correlate the experimental binding constants (or binding free energy and enthalpy) to newly available force measurements [6, 34].

There are attempts to exploit the force detection capability of AFM as a new type of biosensor. Baselt *et al*. [3] are constructing a new sensor that should detect the presence of specific macromolecules at a low concentration of 10^{-18} M range. A piezoresistive cantilever without imaging tip is covered with antibody and dipped in the test solution. Antigens, if present in the solution, bind to the antibodies on the cantilever. The system is then treated with a suspension of small magnetic balls coated with antibodies, thus, allowing the adhesion of magnetic balls to the cantilever only when it has bound antigens. The vibrational

frequency analysis of the cantilever under oscillating magnetic field allows the detection of the presence of even a single ball on the cantilever. It has been tested for streptavidin-biotin system.

Unbinding force between complementary strands of DNA has been the focus of studies by Lee *et al*. [27] and Florin *et al*. [12]. Lee *et al*. [27] used oligonucleotides with the multiple of four bases and measured the rupture force that was calculated from the final jump of the force curve: (1) when the tip and substrate were covered with directly complementary strands with the same length; (2) when the tip and the substrate were coated with the same type of oligonucleotides and bridged with longer strands of complementary base sequences. They used oligonucleotides of different length and found that the combined frequency of rupture force showed multiple peaks around 1.52, 1.11, and 0.83 nN for 20, 16, 12 base pair interactions. The non-specific interaction between non-complementary strands was estimated to be 0.48 nN.

Florin *et al*. [12] studied the force required to separate poly-dA (fixed on agarose beads) from oligo-d$(T)_{21}$ that was linked to AFM tip through tip-BSA-biotin-avidin-DNA system. The force was dependent on the time to keep the tip in contact with the sample surface and a constant value of about 4 nN was obtained when the contact time was longer than 100 seconds. Non-complementary interaction between oligo-d$(T)_{21}$ with poly-dC was negligible. The magnitude of rupture force is considered to be influenced by many factors, quantitative treatment based on single pair interaction was not amenable. In the same paper, Florin *et al*. [12] report the results of cantilever force constant calibration by three different methods. The result will be discussed later under **Cantilever calibration**.

Protein stretching

Protein molecules were intentionally stretched for the first time by Mitsui *et al*. [33] by using AFM. They derivatized a large serum protein called α2-macroglobulin with a cross-linker SPDP (succinimidyl pyridyldithio propionate) and mildly reduced with dithiothreitol to confer 5-6 sulfhydryl groups to the protein surface. The protein was freed of dithiothreitol, and a droplet of its buffered solution was placed on a gold coated mica substrate for a short time, and the surface was extensively washed with protein free buffer. The substrate was then immersed in the same buffer in a liquid cell for AFM. A tip which was similarly coated with gold was then approached in the force calibration mode of AFM. The loading part of the force curve showed a continuous change in its slope, indicating a contact over soft material [46]. The unloading part of the force curve had a similar curvature without downward deflection but occasionally curves with conspicuous downward deflections were obtained, indicating a strong adhesive interaction between the tip and the sample such as the one reproduced in Figure 4.

The downward deflection was interpreted as the result of tensile force of the mechanically stretched protein between the tip and the substrate. The deflection of the cantilever at the final release to the free position was subtracted from the total retraction of z-piezo, and the resulting distance was considered to be the maximum length of stretched protein between the tip and the substrate and termed D_{max}, which distributed around two maxima, one at 150 nm and the other at 300 nm. According to Mitsui *et al*. [33], the first peak corresponded to the extension of a single monomer of the protein and the latter to that of disulfide bonded dimers. A monomer of the protein consists of 1541 amino acid residues, and it is internally cross-linked with 22 disulfide bonds. The maximum theoretical extension of a monomer was estimated to be 200 nm from model building. As shown in Figure 5, the final rupture force distributed from 0-1.75 nN, peaking around 0.75-1 nN. The force in the range of 0.75-1 nN was attributed to the severing of Au-S bond(s) that was linking the protein to either the substrate or tip (see below). In Figure 5, since the frequencies of rupture forces less than 0.25 nN were lumped together, the bar over 0.25 nN does not represent a true peak. Such small forces may correspond to desorption of physisorbed proteins, or to the final steps of gradual unbinding between non-covalently bonded subunits.

As a reference experiment, it was checked that there was only a small attractive interaction between the gold tip and the surface of gold coated mica in buffered solution when the gold surface was freshly prepared and kept in pure water. Moreover, when the sulfhydryl groups on the protein were quenched with a blocking agent, *N*-(7-dimethylamino-4-methylcoumarinyl) maleimide, after immobilization on a gold substrate, force curves stopped exhibiting any significant downward deflections, proving that the force for non-specific adhesion of protein to the tip was negligibly small. It is, therefore, reasonably certain that the downward deflection was due to the presence of tensile protein molecules covalently bonded between the tip and the substrate. The number of protein molecules stretched at a time was not determined but force curves with a simple structure obtained as the active sulfhydryls were progressively quenched with the blocking agent were considered to represent single-molecule stretching events. The spring constant of cantilevers was calibrated by using a standard cantilever constructed from a thin gold wire.

In the experiment of Mitsui *et al*. [33], the system at the molecular level was deliberately kept simple so that the only possible tensile material between the tip and the substrate should be protein. Such a requirement was met at the expense of protection of proteins from possible mechanical deformations. It is, therefore, desirable to check the activity of the protein directly cross-linked to a gold

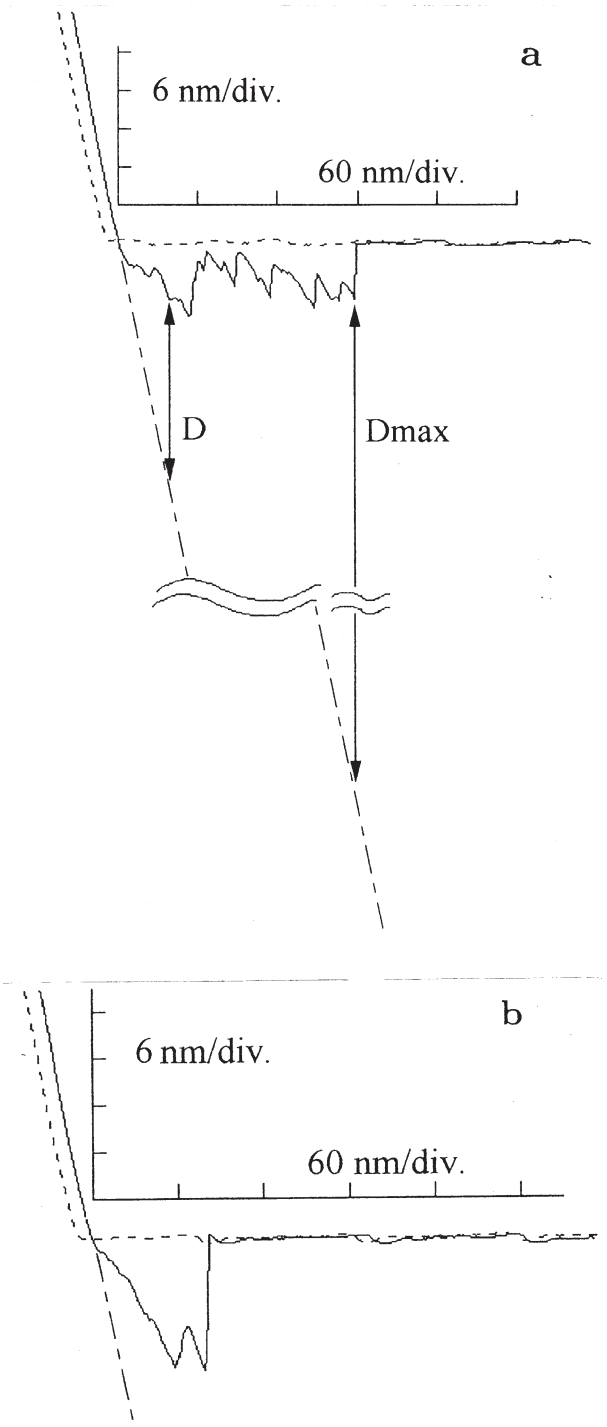

Figure 4. A representative force curve in the stretching experiment of protein. (**a**) Definition of D, and D_{max}, and (**b**) a possible force curve for the stretching of a single protein molecule randomly derivatized with SPDP.

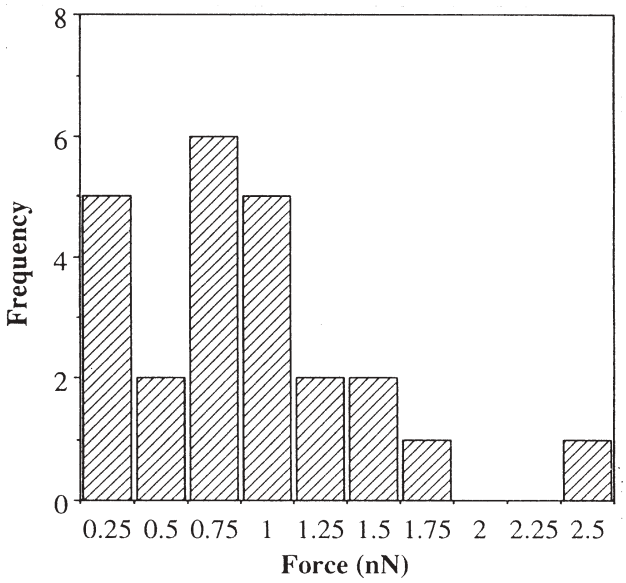

Figure 5. Distribution of force at the end of stretching of a α_2-macroglobulin derivatized with SPDP and sandwiched between the gold coated tip and substrate.

surface to see whether it retained the native structure or not, and to reduce the impact on protein molecules at the time of contact with the AFM tip.

We have recently extended the same experimental procedure to another protein with a simpler structure, namely, bovine carbonic anhydrase B (Mitsui and Ikai, to be published). This protein neither has disulfide bonds nor free cysteine residues and consists of 259 amino acids. In average, 6 lysyl residues were derivatized with SPDP in a similar manner as above. The protein was then immobilized on a gold coated mica in a liquid cell of AFM, and the force curves were taken using a gold coated tip. The distribution of D_{max} had a peak around 30-50 nm, a considerably smaller value compared with the average D_{max} in the experiment on α2-macroglobulin. The unbinding force was centered around 0.7-1.0 nN.

To test our hypothesis that the final rupture force of 0.7-1.0 nN corresponded to the break of an Au-S covalent bond, we conducted the following experiment. A freshly prepared gold surface on mica was reacted with 5 mM aqueous solution of dithiothreitol (*threo*1, 4-dimercapto-2, 3-butanediol) for 5 minutes at 25°C. The gold substrate was subsequently thoroughly washed with distilled water. It was then submerged under a buffer solution, and the force curve was taken using a gold coated tip with a calibrated cantilever. The magnitude of downward deflection at the time of final rupture was converted to force and plotted in Figure 6.

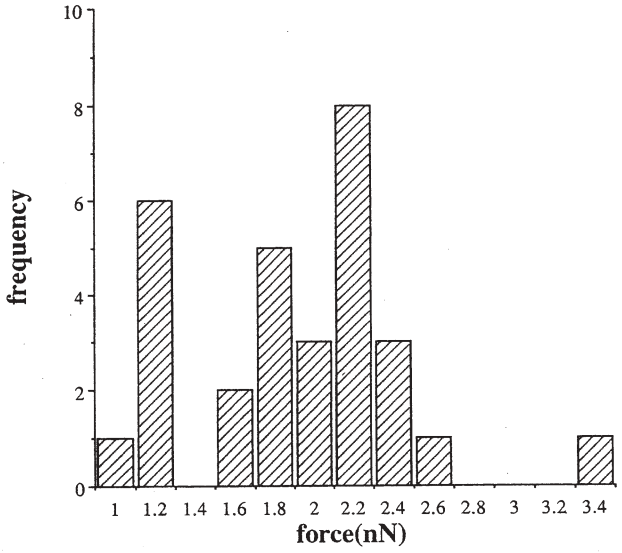

Figure 6. Distribution of rupture force when dithiothreitol was sandwiched between the gold coated tip and the sample.

When the sulfhydryl groups were blocked with DACM {*N*-(7-dimethylamino-4-methyl-3-coumarinyl)-maleimide}, no adhesion was observed. Figure 6 summarizes the distribution of measured force showing two peaks, one in the range of 1-1.1 nN and the other around 2-2.2 nN. We tentatively assume that the first peak corresponds to the rupture of one Au-S bond, and the second to that of two Au-S bonds. More complete experiments are being carried out to establish that the final rupture event in these experiments corresponded to severing of Au-S bonds.

The rupture force of the C-C single bond, which has the dissociation energy of 348 kJ/mol, is predicted to be 5.2 nN based on the Morse function for this bond. The bond energy of N-C single bond is 292 kJ/mol [35]. The bond between the atomic sulfur and gold has been estimated to be approximately 334 kJ/mol [52], which is comparable to the bond energy of C-C bond. The bond energy between the thiolate group and gold surface is about 183 kJ/mol in a vacuum [10, 53] and considerably lower than the above three cases. In the absence of reliable parameters of Morse function for the thiolate-gold bond, it is not easy to estimate the rupture force of the bond. Moreover, our experiment was done in aqueous buffers, and it is possible that the thiolate-gold bond may have different character from vacuum condition. From the above experimental and theoretical considerations, it seems reasonable to assume, at this moment, that the first bond that yielded to the tensile force in Mitsui's experiment was alkanethiolate-gold bonds [33].

We are further extending our experiment to include the stretching of genetically engineered carbonic anhydrase B that has cysteine residues at N- and C-termini. The stretching in this case will be that of from two ends of a linear polymer, and interpretation of the data would be simpler than the preceding cases. The total extended length should be 96 nm assuming the extended length of one amino acid residue is 0.38 nm. Our preliminary experiment indicated that, though the number of successful events is still very small, the force curves in such cases show a D_{max} of about 80-120 nm and the final rupture force of 0.7-0.9 nN, both values being in our expected ranges. The discrepancy between D_{max} and the total length of the protein may be explained that the adhesive bonds are severed before the full extension of the polypeptide.

The biochemical significance of protein stretching experiment may not be as apparent as those of antibody-antigen interactions, or rupture of double helical DNA strands. In fact, there are a number of problems in biochemistry that concerns with the mechanical stability of proteins. To mention a few, transport of globular proteins across a lipid membrane is often accomplished by first unravelling the protein from its one end, let that end cross the membrane with the help of membrane associated system, and then pass the polypeptide chain through the membrane by successively unfolding and refolding it [57, 62, 63]. Another example is the perennial problem of protein folding [51] which, as we think, would be approachable from a different path, once we acquire more data on mechanical unfolding of proteins in addition to a large body of thermodynamic ones. For example, refolding of a once stretched protein would proceed in a more orderly fashion to the correct native form if its N- and C-termini were held at the farthest ends to avoid entanglement during the refolding process. One advantage the AFM has is that such an experiment can be conducted both in aqueous environment and in vacuum allowing more reliable consultations with theoretical predictions, since water presents itself in theoretical studies as a notoriously difficult solvent.

Chromosomes

Application of AFM to biological studies cannot miss the opportunity to image and manipulate chromosomes. The most popular subject of investigation in this field has been the metaphase chromosomes with the well known banding patterns after Giemsa staining. The banding patterns have been reproduced in AFM images of acetic acid: methanol treated chromosomes suggesting that the bands are reflections of not only the chemical nature but also topographical features of the chromosome [37]. Acid treatment of chromosomes is a standard method to prepare them for the study with fluorescence and optical

microscopes, including the powerful new technique of fluorescence *in situ* hybridization (FISH) and the banding pattern in such DNA after Giemsa staining has been regarded to represent the biased localization of DNA with different base compositions [61] and differential folding path of adenine-thymine rich scaffold [30, 49, 50]. Nucleosomal sub-structure of chromosomes was observed with AFM on the preparation obtained after hypotonically treating chicken erythrocytes [13, 14, 15]. Therefore, it is, basically possible to bring the AFM tip to the desired position of chromosomes and nucleosomes with a better precision than hitherto accomplished with other methods.

Rasch *et al*. [48] imaged human metaphase chromosomes hybridized with biotinylated probe DNA. They reported that the hybridized sites of the chromosomes treated with acetic acid and alcohol showed precipitation of certain crystals. The identity of the precipitate was speculated as the reaction products between the enzyme, peroxidase, which was conjugated to probe DNA with avidin, and its substrate, diaminebenzidine. The enzyme:substrate system was adopted for the color generation in the proximity of probe sites. It is convenient if it is possible to identify the hybridized sites by AFM for the later manipulation. A similar work has been reported by De Grooth and Putman [9]. For other works of interest on chromosomes see references [32, 42].

Manipulation of chromosomes using a laser ablation method has been cultivated to isolate genetic materials from restricted regions of chromosomes [16, 66]. In principle and in practice, it is now possible to amplify a single copy of DNA using PCR (polymerase chain reaction) method for sequence determination. Therefore, it is an interesting and ambitious attempt to isolate a single copy of DNA from a preselected region of chromosomes and amplify and sequence it. So far, there has been no reports of successful use of AFM to isolate selected regions of chromosomes and amplify them for sequencing. One attempt in that direction was reported by Mosher *et al*. [36], who used AFM to first image the sample and then in the middle of the next scan the force was increased while arresting the tip in the same scan line. The region of the chromosome was clearly dissected with a width of several tens of nanometers. Recovery of DNA from the dissected region was not clearly demonstrated. The major problem of this method is that the dissection is done along a straight line crossing the entire width of a chromosome. It is not possible to limit the dissection to spatially confined area in two dimensions. In this respect, a better method must be developed which, for example, confine the contact of tip and chromosome to a region of the order of 10 nm x 10 nm and cross-link the tip and DNA while they are in touch with each other and then increase the distance between the tip and the chromosome as in the force curve measurement mode.

Manipulation of chromosomes has an important advantage over nanometric manipulation of other subcellular structures in that the effect of manipulation may be biologically amplified if the engineered chromosomes remain native. Acid treated chromosomes are not suitable for such purposes except in an early stage of trial. Chromosomes without denaturing treatment must be prepared and manipulated and replaced in the cell afterward to see the biological effects of manipulation.

Cantilever calibration

In all types of force measurements, calibration of cantilevers for their force constant is prerequisite. There are several proposed methods of this procedure as listed below. Each method will be briefly explained with details referred to cited literature.

Natural vibrational frequency The cantilever natural frequency itself is related to its spring constant through the following equation:

$$k = m_{\text{eff}} \text{ x } (2\pi\nu)^2 \qquad (6)$$

In the above equation, m_{eff} is the effective mass of the cantilever and approximately equal to 0.24 x m_b, where m_b is the mass of a rectangular beam [7]. When the cantilever is a V-shaped one, it is approximated by two rectangular cantilevers with equal length [5]. By measuring the resonance frequency of a test cantilever in the cantilever tuning mode of AFM, it is possible to obtain the spring constant, *k*. In practice, the resonance curve of AFM tuning gives multiple peaks because most of commercially available cantilevers have a triangular shape and even the dominant peak is rather broad, making it difficult to determine the resonant frequency with required accuracy.

Vibrational frequency of loaded cantilever Cleveland *et al*. [7] devised a clever method of changing the mass of a cantilever by sequentially adding tungsten balls to the edge of a test cantilever and measuring the resonance frequencies as a function of the total mass of the cantilever. The slope of the plot between $2\pi\nu^2$ and the mass of the tungsten balls gives an accurate measure of *k*. The procedure is an admirable one but it requires time to calibrate several cantilevers in this way. The same method was used by Noy *et al*. [39] when they developed a chemical force microscopy which was used to probe the chemically distinct characteristics of the self-assembled monolayer surface with AFM.

Power spectrum of thermal vibration The vibration of free cantilever due to thermal noise can be recorded on a standard AFM. The average of squared amplitude of vibration, $\langle(\Delta x)^2\rangle$ is related to the thermal energy k_BT through:

$$\frac{1}{2}k < (\Delta x)^2 >= \frac{1}{2}k_B T \qquad (7)$$

where k, k_B and T represent, the cantilever spring constant, the Boltzmann constant, and the absolute temperature. $<(\Delta x)^2$ can be obtained from the power spectrum of noise amplitude of unloaded cantilever. The method was applied to AFM cantilever calibration by Hutter and Bechhoefer [23]. Figure 7 shows such a power spectrum reproduced from reference [23]. This method neither requires any modification of the AFM nor additional major equipment, and is thus recommended by several workers.

Use of calibrated spring Hinterdorfer *et al*. [20] acquired calibrated AFM cantilevers from a manufacturer of AFM instrument and used it to obtain standard force curves and calculated the spring constant of test cantilevers. The spring constant of a test cantilever can be obtained by comparing the slopes of the force curves obtained on a glass surface and on the reference cantilever. In other cases, standard cantilevers were constructed from a piece of glass fiber of thin gold wire with cylindrical cross-section of known diameters [29, 33]. Li *et al*. [29] determined the spring constant they used in the measurement of the force acting between colloidal particles by pressing a piece of glass fiber whose spring constant was pre-calibrated from measuring its deflection when loaded with a small load. After calibrating the spring constant of such cantilevers, they were used for calibration standard of test AFM cantilevers. This method is recommended because it relies on few assumptions. The spring constant of a cylindrical cantilever with diameter d and length l and made of a material with Young's modulus E can be calculated by the following equation.

$$k = \frac{3\pi E d^4}{64 l^3} \qquad (8)$$

Florin *et al*. [12] used a hand-made polymer spring 35 mm in length with a rectangular cross-section (2 mm x 0.1 mm) as a reference cantilever. It was cut out from an overhead projector sheet and calibrated for its spring constant by loading a known weight.

Use of calibrated pendulum Butt *et al*. [5] used a finely tuned pendulum for calibration of their cantilever. The deflection of a vertically positioned cantilever, when it was pressed against the pendulum, was accurately measured by using a telescope and the force was determined from the deflection of the pendulum from its free vertical position.

Use of compound of known elastic property Some early investigators used material such as rubber as one of the calibration standards in force curve measurement [59]. It is convenient if an elastic material with constant elastic property is always available. It is recommended to measure spring constant of a test cantilever in aqueous salt solution to avoid electrostatic interactions between the tip and the reference material.

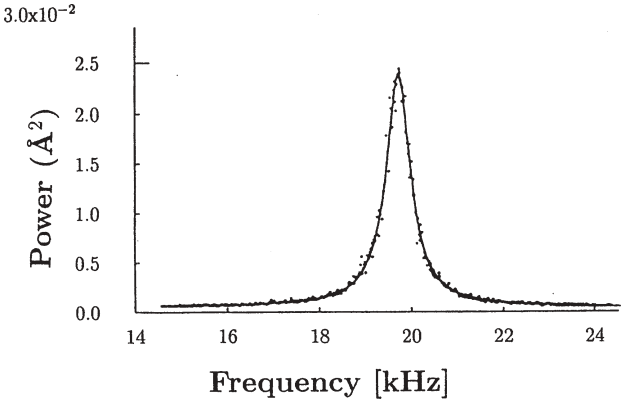

Figure 7. Power spectrum of thermal vibration of a test cantilever as adapted from Hutter and Bechhoefer [23].

Direct measurement of cantilever deflection due to end-loading of tungsten balls Senden and Ducker [54] measured the deflection of AFM cantilever with a small tungsten ball loaded at its end. By knowing the diameter and the density of the tungsten ball, and the magnitude of cantilever deflection from the optical lever system of AFM, they calculated the spring constant of commercial silicon nitride cantilevers. Their measurement showed that there was up to 300% difference between the nominal spring constant supplied by the manufacturer and the measured values. Calculated values from the cantilever geometry could be different from the measured ones by a factor of 2, due probably, to the difference in Young's modulus of the non-stoichiometric silicon nitride.

Florin *et al*. [12] compared the result obtained by using three methods, thermal noise method, use of a calibrated cantilever, and resonance frequency method, for calibrating test cantilevers. They reported that there was a 1.8 times difference in the spring constant among commercially microfabricated cantilevers taken from the same batch, and 20% difference among the spring constants determined for the same cantilevers by the three methods. The authors recommended the thermal vibration method for its simplicity and especially for the calibration of soft cantilevers.

Conclusions

The usefulness of nanometer level mechanical parameters in contemporary biology is yet to be established.

Not only in biochemistry but in chemistry in general, quantitation of molecular interactions and stability of macromolecular complexes has been described in terms of the binding constant and free energies, i.e., with the language of thermodynamics. This article reviewed a new trend in biochemistry and biophysics to characterize such interactions in terms of force rather than energy.

Acknowledgements

We are indebted to Dr. Masahiko Hara of Riken Institute for his help in preparation of gold coated mica substrates and for valuable discussions. We also express our sincere gratitude to Professor Kikuo Kishimoto of Tokyo Institute of Technology for his valuable advice in the fundamentals and recent development of material mechanics. We thank Professor Kin Ping Wong of the California State University at Fresno for his gift of cloned gene of bovine carbonic anhydrase B. Financial supports from the Ministry of Education through a Grant-in-Aid for Priority Research to A.I. and a grant from New Energy and Industrial Technology Development Organization are appreciated.

References

[1] Aimé JP, Elkaakour Z, Odin C, Bouhacina T, Michel D, Curély J, Dautant A (1994) Comments on the use of the force mode in atomic force microscopy for polymer films. J. Appl. Phys. **76**, 754-762.

[2] Baljon ARC, Robbins MO (1996) Energy dissipation during rupture of adhesive bonds. Science **271**, 482-484.

[3] Baselt DR, Lee GU, Colton RJ (1996) Biosensor based on force microscope technology. J. Vac. Sci. Technol. **B14**, 789-793.

[4] Burnham NA, Colton RJ (1989) Measuring the nanomechanical properties and surface forces of materials using an atomic force microscope. J. Vac. Sci. Technol. **A7**, 2906-2913.

[5] Butt HJ, Siedle P, Seifert K, Fendler K, Seeger T, Bamberg E, Weisenhorn AL, Goldie K, Engel A (1993) Scan speed limit in atomic force microscopy. J. Microsc. **169**, 75-84.

[6] Chilkoti A, Boland T, Ratner BD, Stayton PS (1995) The relationship between ligand-binding thermodynamics and protein ligand interaction forces measured by atomic force microscopy. Biophys. J. **69**, 2125- 2130.

[7] Cleveland JP, Manne S, Bocek D, Hansma PK (1993) A nondestructive method for determining the spring constant of cantilevers for scanning force microscopy. Rev. Sci. Instrum. **64**, 403-405.

[8] Dammer U, Hegner M, Anselmetti D, Wagner P, Dreier M, Huber W, Güntherodt HJ (1996) Specific antigen/antibody interactions measured by force microscopy. Biophys. J. **70**, 2437-2441.

[9] De Grooth BG, Putman CAJ (1992) High-resolution imaging of chromosome-related structures by atomic force microscopy. J. Microsc. **168**, 239-247.

[10] Dubois LH, Nuzzo RG (1992) Synthesis, structure and properties of model organic surfaces. Annu. Rev. Phys. Chem. **43**, 437-463.

[11] Florin EL, Moy VT, Gaub HE (1994) Adhesion forces between individual ligand-receptor pairs. Science **264**, 415-417.

[12] Florin EL, Rief M, Lehmann H, Ludwig M, Dornmair C, Moy VT, Gaub HE (1995) Sensing specific molecular interactions with the atomic force microscope. Biosensors Bioelectron. **10**, 895-901.

[13] Fritzsche W, Henderson E (1996) Ultrastructural characterization of chicken erythrocyte nucleosomes by scanning force microscopy. Scanning **18**, 138-139.

[14] Fritzsche W, Schaper A, Jovin TM (1994) Probing chromatin with the scanning force microscope. Chromosoma **103**, 231-236.

[15] Fritzsche W, Schaper A, Jovin TM (1995) Scanning force microscopy of chromatin fibers in air and in liquid. Scanning **17**, 148-155.

[16] Hadano S, Watanabe M, Yokoi H, Kogi M, Tsuchiya H, Kanazawa I, Wakasa K, Ikeda J (1991) Laser microdissection and single unique primer PCR allow generation of regional chromosome DNA clones from a single human chromosome. Genomics **11**, 364-373.

[17] Hansma HG, Hoh JH (1994) Biomolecular imaging with the atomic force microscope. Annu. Rev. Biophys. Biomol. Struct. **23**, 115-139.

[18] Henderson E (1994) Imaging of living cells by atomic force microscopy. Prog. Surf. Sci. **46**, 39-60.

[19] Hendrix BC (1995) The use of shape correction factors for elastic indentation measurements J. Mater. Res. **10**, 255-257.

[20] Hinterdorfer P, Baumgartner W, Gruber HJ, Schilcher K, Schindler H (1996) Detection and localization of individual antigen-antibody recognition events by atomic force microscopy. Proc. Natl. Acad. Sci. (USA) **93**, 3477-3481.

[21] Hoh JH, Hansma P (1992) Atomic force microscopy for high-resolution imaging in cell biology. Trends Cell Biol. **2**, 208-213.

[22] Hoh JH, Schoenenberger C-A (1994) Surface morphology and mechanical properties of MDCK monolayers by atomic force microscopy. J. Cell Sci. **107**, 1105-1114.

[23] Hutter JL, Bechhoefer J (1993) Calibration of atomic force microscope tips. Rev. Sci. Instrum. **64**, 1868-1873.

[24] Ikai A, Mitsui K, Tokuoka H, Xu XM (1997) Mechanical measurement of a single protein molecule and human chromosomes by atomic force microscopy. Mater. Sci. Eng. **C4**, 233-240.

[25] King RB (1987) Elastic analysis of some punch problems for a layered medium. Int. J. Solids Struct. **23**, 1657-1664.

[26] Lee WA, Peacocke AR (1951) Electrometric titration of the sodium salts of deoxyribonucleic acids. J. Chem. Soc. Part 4, 3361-3371.

[27] Lee GU, Chrisey LA, Colton RJ (1994) Direct measurement of the forces between complementary strands of DNA. Science **266**, 771-773.

[28] Lee GU, Kidwell DA, Colton RJ (1994) Sensing discrete streptavidin-biotin interactions with AFM. Langmuir **10**, 354-357.

[29] Li YQ, Tao NJ, Pan J, Garcia AA, Lindsay SM (1993) Direct measurement of interaction forces between colloidal particles using the scanning force microscope. Langmuir **9**, 637-641.

[30] Ma X, Saitoh N, Curtis PJ (1993) Purification and characterization of a nuclear DNA-binding factor complex containing topoisomerase 11 and chromosome scaffold protein 2. J. Biol. Chem. **268**, 6182-6188.

[31] Marti O (1993) SXM: An introduction. In: STM and SFM in Biology. Marti O, Amrein M (eds.). Academic Press, Inc., New York, N.Y. Chap. 1.

[32] McMaster TJ, Hickish T, Min T, Cunningham O, Miles MJ (1994) Application of scanning force microscopy to chromosome analysis. Cancer Genet. Cytogenet. **76**, 93-95.

[33] Mitsui K, Hara M, Ikai A (1996) Mechanical stretching of alpha-2-macroglobulin molecules with atomic force microscope. FEBS Lett. **385**, 29-33.

[34] Miyamoto S, Kollman PA (1993) What determines the strength of noncovalent association of ligands to proteins in aqueous solution? Proc. Natl. Acad. Sci. (USA) **90**, 8402-8406.

[35] Moore WJ (1972) Physical Chemistry (4th ed.). Prentice Hall, Englewood Cliffs, N.J. Chap. 2.

[36] Mosher C, Jondle D, Ambrosio L, Vesenka J, Henderson E (1994) Microdissection and measurement of polytene chromosomes using the atomic force microscope. Scanning Microsc. **8**, 491-497.

[37] Musio A, Mariani T, Frediani C, Sbrana I, Ascori C (1994) Longitudinal patterns similar to G-banding in untreated human chromosomes: Evidence from atomic force microscopy. Chromosoma **103**, 225-229.

[38] National Astronomical Society of Japan (1996) Chronological Scientific Tables, Maruzen Co., Tokyo. p. 446. (In Japanese).

[39] Noy A, Frisbie CD, Rozsnyai LF, Wrighton MS, Lieber CM (1995) Chemical force microscopy: Exploiting chemically-modified tips to quantify adhesion, friction, and functional group distribution in molecular assemblies. J. Am. Chem. Soc. **117**, 7943-7951.

[40] Oliver WC, Pharr GM (1992) An improved technique for determining hardness and elastic modulus using load and displacement sensing indentation experiments. J. Mater. Res. **7**, 1564-1583.

[41] Pharr GM, Oliver WC, Brotzen FR (1992) On the generality of relationship among contact stiffness, contact area and elastic modulus during indentation. J. Mater. Res. **7**, 613-617.

[42] Putman CAJ, de Grooth BG, Wiegant J, Rapp AK, Van der Werf KO, Van Hulst NF, Greve J (1993) Detection of *in situ* hybridization to human chromosomes with the atomic force microscope. Cytometry **14**, 356-361.

[43] Radmacher M, Tillmann RW, Fritz M, Gaub HE (1992) From molecules to cells: Imaging soft samples with the atomic force microscopes. Science **257**, 1900-1905.

[44] Radmacher M, Tillmann RW, Gaub HE (1993) Imaging viscoelasticity by force modulation with the atomic force microscope. Biophys. J. **64**, 735-742.

[45] Radmacher M, Cleveland JP, Fritz M, Hansma HG, Hansma PK (1994) Mapping interaction forces with the atomic force microscope. Biophys. J. **66**, 2159-2165.

[46] Radmacher M, Fritz M, Cleveland JP, Walters DA, Hansma PK (1994) Imaging and adhesion forces and elasticity of lysozyme adsorbed on mica with the atomic force microscopy. Langmuir **10**, 3809-3814.

[47] Radmacher M, Fritz M, Hansma PK (1995) Imaging soft samples with the atomic force microscope: Gelatin in water and propanol. Biophys. J. **69**, 264-270.

[48] Rasch P, Wiedemann U, Wienberg J, Heckl WM (1993) Analysis of banded human chromosomes and *in situ* hybridization patterns by scanning force microscopy. Proc. Natl. Acad. Sci. (USA) **90**, 2509-2511.

[49] Saitoh Y, Laemmli UK (1994) Metaphase chromosome structure: Bands arise from a differential folding path of the highly AT-rich scaffold. Cell **76**, 609-622.

[50] Saitoh N, Goldberg IG, Wood ER, Earnshaw WC (1994) ScII: An abundant chromosome scaffold protein is a member of a family of putative ATPase with an unusual predicted tertiary structure. J. Cell Biol. **127**, 303-318.

[51] Shultz GE, Shirmer RH (1978) Principle of Protein Structure. Springer Verlag, New York. Chap. 5.

[52] Sellers H (1993) On the chemisorption and dissociation of $HSCH_3$ on the Au(111) surface. Surf. Sci. **294**, 99-107.

[53] Sellers H, Ulman A, Shnidman Y, Eilers JE (1993) Structure and binding of alkane thiolates on gold and silver surfaces: Implication for self-assembled monolayers. J. Am. Chem. Soc. **115**, 9389-9401.

[54] Senden TJ, Ducker WA (1994) Experimental

determination of spring constants in atomic force microscopy. Langmuir **10**, 1003-1004.

[55] Shao Z, Yang J, Somlyo AP (1995) Biological atomic force microscopy: From microns to nanometers and beyond. Annu. Rev. Cell Dev. Biol. **11**, 241-265.

[56] Sneddon IN (1965) The relation between load and penetration in the axisymmetric Boussinesq problem for a punch of arbitrary profile. Int. J. Eng. Sci. **3**, 47- 57.

[57] Stuart RA, Cyr DM, Craig EA, Neupert W (1994) Mitochondrial molecular chaperones: Their role in protein translocation. Trends Biol. Sci. **19**, 87-92.

[58] Sugahara Y, Ohta M, Ueyama H, Morita S (1995) Defect motion on an InP(110) surface observed with noncontact atomic force microscopy. Science **270**, 1646-1648.

[59] Tao NJ, Lindsay SM, Lees S (1992) Measuring the microscopic properties of biological materials. Biophys. J. **63**, 1165-1169.

[60] Treloar LRG (1975) The Physics of Rubber Elasticity. Clarendon Press, Oxford, U.K. pp. 142-143.

[61] Van Holde KE (1988) Chromatin. Springer-Verlag, New York. Chap. 7.

[62] Walter P, Johnson AE (1994) Signal sequence recognition and protein targeting to the endoplasmic reticulum membrane. Annu. Rev. Cell Biol. **10**, 87-119.

[63] Wickner W, Driessen A, Hartle F-U (1991) The enzymology of protein translocation across the *Escherichia coli* plasma membrane. Annu. Rev. Biochem. **60**, 101-124.

[64] Xu XM, Ikai A (1997) Measuring nanoelasticity of human chromosomes using the atomic force microscope. Cell. Eng. **2**, 75-81.

[65] Xu W, Mulhern PJ, Blackford BL, Jericho MH, Templeton I (1994) A new force microscopy technique for the measurement of the elastic properties of biological materials. Scanning Microsc. **8**, 499-506.

[66] Yokoi H, Hadano S, Kogi M, Kang X, Wakasa K, Ikeda J (1994) Isolation of expressed sequences encoded by the human Xq terminal portion using microclone probes generated by laser microdissection. Genomics **20**, 404-411.

Discussion with Reviewers

Reviewer II: Please discuss the effect of the weak cantilever for which the sensitivity for sample properties are destroyed as soon as the force curve becomes linear.

Authors: The force curve taken with very soft cantilever may not reveal the elastic properties of the sample. Then, we have to replace the cantilever with a slightly stronger one and see if the new cantilever reveals more about the sample. It is happening to us now, as we work on seemingly harder proteins. The dynamic range of force measurement of AFM is rather limited if one sticks to one cantilever.

M. Radmacher: The Young's modulus reported by Xu *et al.* [65] for a chitin fiber (100-200 GPa) is surprisingly high. It is actually larger than that of glass (70 GPa) and comparable to steel (200 GPa). This is the highest value I have ever heard for biological material, even spider silk has only a Young's modulus of about 10 GPa. Please comment on this?

Authors: We agree with you that the value for chitin is very high. We are not familiar with this material, and therefore contacted the original authors and obtained their present position on the results. Dr. Jericho (personal communication, 1997) stated that they obtained lower value of Young's modulus for larger beams than the one we cited, but for smaller ones, the Young's modulus was still high. He admits that, for its highly crystalline structure, β-chitin is expected to have a large Young's modulus, but the value in the order of 100 GPa could be an overestimate; so far, there is no obvious reason for such overestimation.

M. Radmacher: The chromosomes were dehydrated with methanol and acetic acid before their elastic properties were investigated in various buffers. This is a potentially denaturing process. Do you know how much the elastic properties are modified by this procedure? Have you tried to investigate the chromosomes in their native form?

Authors: You are perfectly correct in that the acetic acid:methanol treatment of chromosomes is quite denaturing, in fact, it extracts most of histones, leaving only a minor protein called scaffold protein. We are sure the procedure changed the mechanical properties of chromosomes very much. Most of the biological work such as localization of specific genes using fluorescence *in situ* hybridization (FISH) is done on such chromosomes. Our initial aim in this study was to obtain the mechanical parameters of such chromosomes to start manipulating on the same type of chromosomes as used in FISH experiments. We are now trying to prepare chromosomes in more native conditions.

M. Radmacher: During the swelling of chromosomes you observe a drastic change in height as well in the apparent width. Higher features will automatically appear broader due to the pyramidal shape of the tips. Might the change in width be due to tip broadening?

Authors: It certainly is possible. From the value of Young's modulus determined in our experiment, we estimated that during the scanning process for imaging, chromosomes were depressed up to 200 nm by the applied scanning force. We must take what you said into account when we measure the volume of the chromosomes.

M. Radmacher: A possible proof of specific events like single covalent bonds being broken would be peaks in the

force distribution at integral multiples of a force quanta. Have you observed this quantization? Have you tried to prove the proposed covalent nature of the rupture forces? For example, covalent forces should be independent of the environment, like pH and salt concentrations.
Authors: In our new experiment on dithiothreitol, yes we have. It is a valuable suggestion from you to measure rupture force at different pH's although there is a possibility that the thiolate-Au bonding may be influenced by pH of the buffer if one considers the possibility of proton based catalysis of the rupture.

T. Mariani: When you say the height of the chromosomes are 100-200 nm, do you mean the range of variation or the uncertainty in the measurement, and when you give the numerical data in the form of x ± y, does "y" mean the standard deviation?
Authors: In the case of chromosome height measurement, especially for the dried sample, the height measurement referred to as 100-200 nm means the uncertainty range between sample to sample. The drying process was evidently not well controlled. When the data is given as x ± y, yes, y means standard deviation.

W. Fritzsche: Fixation of biological samples is often based on a cross-linkage of the specimen material to reach high mechanical stability. Such fixation probably influences Young's modulus. What is your opinion about difference of this parameter in native compared to fixed chromosomes?
Authors: In the case of chromosomes, fixation with acetic acid and methanol comes from the necessity to dispose of the cell debris covering the chromosomal surface, resulting in the extraction of most of the intrinsic protein components of chromosome itself. We are sure that such fixation procedure greatly changed the mechanical properties of chromosomes. The fixation procedure probably changed chromosomes into a highly elastic gel-like material from the more compactly folded nucleo-protein complexes.

W. Fritzsche: The metaphase chromosome exhibits probably a longitudinal core-like structure (the suggested protein scaffold structure) surrounded by peripheral region of chromatin loops. Could you find any differences in Young's modulus with respect to the (radial) location you measured, pointing to different mechanical parameters of these two regions?
Authors: From the images of metaphase chromosomes, there seems to be the structure that you mention, but our force curve measurements could not distinguish the mechanical properties of the two regions. Perhaps with more careful experimentation, we would be able to find the difference.